Electrochemical exfoliation of graphite in aqueous sodium halide electrolytes towards low oxygen content graphene for energy and environmental applications

J.M. Munuera[a*], J.I. Paredes[a], M. Enterría[b], A. Pagán[c], S. Villar-Rodil[a], M.F.R. Pereira[b], J.I. Martins[d,e], J.L. Figueiredo[b], J.L. Cenis[c], A. Martínez-Alonso[a], J.M.D. Tascón[a]

[a]*Instituto Nacional del Carbón, INCAR-CSIC, Apartado 73, 33080 Oviedo, Spain*
[b]*Laboratório de Processos de Separação e Reacção – Laboratório de Catálise e Materiais (LSRE-LCM), Departamento de Engenharia Química, Faculdade de Engenharia, Universidade do Porto, R. Dr. Roberto Frias s/n, 4200-465 Porto, Portugal*
[c]*Instituto Murciano de Investigación y Desarrollo Agrario y Alimentario (IMIDA), Calle Mayor 1, 30150 La Alberca, Spain*
[d]*Departamento de Engenharia Química, Faculdade de Engenharia, Universidade do Porto, R. Dr. Roberto Frias s/n, 4200-465 Porto, Portugal*
[e]*Universidade do Minho, LAB2PT- Laboratório de Paisagens, Património e Território, Portugal*

Abstract

Graphene and graphene-based materials have shown great promise in many technological applications, but their large-scale production and processing by simple and cost-effective means still constitute significant issues in the path of their widespread implementation. Here, we investigate a straightforward method for the preparation of a ready-to-use and low oxygen content graphene material that is based on electrochemical (anodic) delamination of graphite in aqueous medium with sodium halides as the electrolyte. Contrary to previous conflicting reports on the ability of halide anions to act as efficient exfoliating electrolytes in electrochemical graphene exfoliation, we show that proper choice of both graphite electrode (e.g., graphite foil) and sodium halide concentration readily leads to the generation of large quantities of single-/few-layer graphene nanosheets possessing a degree of oxidation (O/C ratio down to ~0.06) lower than that typical of anodically exfoliated graphenes obtained with commonly used electrolytes. The halide anions are thought to play a role in mitigating the oxidation of the graphene lattice during exfoliation, which is also discussed and rationalized. The as-exfoliated graphene materials exhibited a three-dimensional morphology that was suitable for their

Keywords: graphene, electrochemical exfoliation, supercapacitors, environmental applications, sodium halides

practical use without the need to resort to any kind of post-production processing. When tested as dye adsorbents, they outperformed many previously reported graphene-based materials (e.g., they adsorbed ~920 mg g^{-1} for methyl orange) and were useful sorbents for oils and non-polar organic solvents. Supercapacitor cells assembled directly from the as-exfoliated products delivered energy and power density values (up to 15.3 Wh kg^{-1} and 3220 W kg^{-1}, respectively) competitive with those of many other graphene-based devices, but with the additional advantage of extreme simplicity of preparation.

1. Introduction

Since its first isolation in 2004, graphene has spurred enormous interest in the scientific community due to its excellent electronic, mechanical, thermal and optical properties, as well as to its wide range of potential applications in many fields, including electronics, photonics, energy conversion/storage, catalysis and biomedicine.[1] However, one of the most pressing issues that hinder the actual implementation and widespread use of graphene is that related to its large-scale production. At present, there is no single method that can simultaneously provide high amounts of material of good quality in a reasonable amount of time at a low cost. The existing production methods can be classified into two types: bottom-up and top-down. The former relies on synthesizing graphene sheets from small-molecule precursors, usually following chemical vapor deposition (CVD) methodologies and giving rise to large-area sheets.[2] Top-down methods, on the other hand, rely on the exfoliation of graphitic materials into single- and/or few-layer graphene flakes. Even though there exists a number of exfoliation strategies, the most relevant ones are arguably (i) the graphite oxide route, (ii) the direct liquid-phase exfoliation method and (iii) the electrochemical exfoliation approach.[3,4] The graphite oxide strategy involves harsh oxidation of graphite, causing the oxidized basal planes to be easily exfoliated in polar solvents (including water) into single-layer graphene oxide by sonication or other means.[5] This oxidation can be partially reversed through a reduction process, but the resulting product (reduced graphene oxide) always retains significant amounts of oxygen and structural defects.[6] Direct liquid-phase exfoliation generally circumvents oxidation issues because delamination is directly promoted via, e.g., ultrasound waves or high-shear forces

in a medium that can colloidally stabilize the graphene flakes (organic solvents, aqueous surfactant solutions, etc).[7] The main drawbacks of this method are the predominance of several-layer or even multilayer graphene flakes rather than single- or few-layer (<4) objects, as well as its low production yield (typically below 5 wt%).

On the other hand, electrochemical (or electrolytic) exfoliation methods are based on the intercalation of ions between the layers of a graphite electrode due to the flow of electrical current in an electrolytic cell. [8,9] These ions induce expansion of the interlayer space in graphite and thus facilitate the exfoliation process. There are essentially two approaches to electrochemical exfoliation, namely, the cathodic and the anodic approach. In the former case, graphite acts as the cathode in the electrochemical cell and intercalates cations from the electrolyte. Studies in this area have been typically carried out in organic solvents with lithium or alkylammonium salts,[10,11] as well as molten salts[12,13] and ionic liquids as the electrolyte,[14] and the obtained products are usually few-layer to several-layer graphene flakes of a high structural quality. Anodic exfoliation, on the other hand, takes place with the graphite material as the anode and is typically accomplished in aqueous electrolytes, which is advantageous from an environmental and practical standpoint.[15,16,17,18] Some studies have also reported the possibility of simultaneous anodic and cathodic exfoliation.[19,20,21] One of the main issues regarding aqueous anodic exfoliation, though, is related to the fact that graphite is subjected to a large positive voltage (typically between a few and a few tens of volts).[8] This voltage induces the formation of highly reactive oxygen species (e.g., hydroxyl radicals) from the oxidation of water molecules, which in turn trigger a significant oxidation and structural degradation the carbon lattice.[8,15]

Due to the well-known ability of the sulfate anion to intercalate graphite, sulfuric acid is widely employed as an electrolyte in the preparation of graphene flakes by anodic exfoliation.[16,17,22,23,24] However, the highly acidic nature of this electrolyte is especially conducive to obtaining graphene flakes with a considerable extent of oxidation (typical O/C atomic ratios in the ~0.10-0.25 range). Other protic acids, such as phosphoric, oxalic or perchloric acids have also been explored, with similar results. [23,25] Use of the corresponding inorganic and organic salts of these acids (e.g., sodium sulfate, citrate or perchlorate) as electrolytes has been proposed as a way to mitigate oxidation of the exfoliated graphenes, but these efforts have met with varied success.[17,22,26] More recently, novel strategies to

prevent graphene oxidation during anodic exfoliation have been explored.[27] For example, exfoliation has been accomplished with standard electrolytes (e.g., sulfuric acid) in the presence of certain additives that inhibit graphene oxidation, such as melamine,[28] or the antioxidants sodium borohydride, ascorbic acid and (2,2,6,6-tetramethylpiperidin-1-yl)oxyl (TEMPO).[29] Likewise, some sulfonated aromatic compounds have been simultaneously used as electrolytes and oxidation-preventing agents for the production of low oxygen content graphene flakes.[30] In these cases, graphenes with O/C atomic ratios down to ~0.02-0.04 were attained. However, such methods suffer from some drawbacks, including the use of relatively expensive additives/electrolytes and the difficulty in removing adsorbed additives/electrolytes from the exfoliated products to obtain neat graphenes (the additives can also induce functionalization of the flakes). Thus, the availability of anodic exfoliation methods that make use of very simple and inexpensive electrolytes and at the same time afford low oxygen content and additive-free graphenes would be highly desirable, but for the most part such methods are currently lacking.

We hypothesized that some very simple salts such as sodium halides (NaCl, NaBr, NaI) could be effective, additive-free electrolytes for the anodic exfoliation of graphite into graphene flakes with a limited extent of oxidation. This idea was supported by the fact that graphitic materials can be intercalated with halogens/halides through electrochemical and other means,[31] so that anodic exfoliation of a graphite electrode could in principle be possible in the presence of halide-based electrolytes. Although alkali halides have been previously used as additives in the preparation of graphene via direct ultrasound-induced exfoliation,[32] there are conflicting reports as to the ability of halide anions to act as efficient electrolytes in the aqueous anodic exfoliation of graphite.[16,17,33] We also note that because halide anions are relatively prone to oxidation, these intercalated species could act as sacrificial agents and neutralize the oxygen radicals generated under anodic potential, thus mitigating the oxidation of the graphene flakes in comparison with other commonly used electrolytes, but this point has not yet been demonstrated.

We have thus investigated the use of sodium halides as electrolytes for the aqueous anodic exfoliation of graphite, the results of which are reported here. Significantly, the production of single- and few-layer graphene flakes with a limited degree of oxidation, and thus of a high structural quality, was made possible by chosing an appropiate graphite

material as the anode and carefully testing different electrolyte concentrations in order to find the intermediate range where exfoliation is succesful. Considering the potential scalability of this method together with the use of sustainable and widely available electrolytes, and that no additives are required to limit oxidation, the present work should broaden the prospects of anodic exfoliation as a competitive method for the large-scale production of single-/few-layer graphene flakes towards different applications, particularly in energy- and environment-related fields. Indeed, we demonstrate the use of the halide-derived, as-exfoliated foam-like graphene products as efficient adsorbents for dyes and oils as well as electrodes for supercapacitors. Also, the biocompatibility of these graphene nanosheets is attested.

2. Results and discussion

2.1. Key aspects of the electrochemical exfoliation of graphite in aqueous halide-based electrolytes

We aimed at determining whether some very simple and widely available salts, such as the sodium halides NaCl, NaBr and NaI, could be effectively used as electrolytes towards the anodic exfoliation of graphite in aqueous medium to give graphene flakes with a limited extent of oxidation. Some previous experiments had concluded that the anodic exfoliation of graphite using halide-based electrolytes was not even possible.[16,17] On the other hand, a recent work by Munaiah *et al* has suggested that exfoliated products can be obtained, although they possess a considerable degree of oxidation (O/C atomic ratios of ~0.10-20).[33] On the basis of a suite of tests with the aforementioned sodium halides, we found that single-/few-layer graphene flakes could indeed be produced in considerable quantities. It is important to note, though, that effective exfoliation was found to be critically dependent on two main factors, namely, the type of graphite used as the anode and the concentration of sodium halide used as electrolytic medium. To understand the influence of these two factors, as well as some characteristics of the resulting graphene materials that will be discussed below, the basic mechanism underlying the anodic exfoliation process has to be borne in mind. Such a mechanism has been discussed elsewhere[17] and will just be briefly outlined here: first of all, exfoliation occurring at a graphite anode in the presence of common aqueous electrolytes (e.g., H_2SO_4) under typical bias voltage conditions (5-15 V)

is believed to start with the oxidation of grain boundaries and edges of the graphite crystals due to the presence of oxygen radicals (e.g., hydroxyl species) generated through oxidation of water molecules at the anode. This initial oxidation induces an expansion of the interlayer space at the edges, which in turn facilitates the intercalation of the graphite layers with anions from the electrolyte together with water molecules. Subsequent redox processes involving the intercalated species are thought to give rise to gaseous products that exert strong forces on the layers, leading to the expansion and swelling of the graphite anode. As a result, an expanded graphitic material composed of very weakly attached layers is finally formed, which can then be readily separated into individual single- or few-layer graphene flakes in a proper solvent medium by means of low-power ultrasound or shear forces.[17,18]

In anodic exfoliation tests carried out with sodium halides using three different types of graphite, namely, graphite foil, highly oriented pyrolytic graphite (HOPG) and graphite flakes (+10 V applied to graphite anode for 60 min with platinum foil as a counter electrode; see Experimental section), we observed that well-exfoliated graphitic materials colloidally dispersed either in the organic solvent *N*,*N*-dimethylformamide (DMF) or in water using, e.g., the biomolecule flavin mononucleotide (FMN) as a stabilizer[18,34] could only be obtained with the former graphite type. By contrast, just slightly expanded materials that could not be stably suspended in DMF or water/FMN were attained with both HOPG and graphite flakes. This result suggested that the halide anions failed to extensively intercalate and/or expand the HOPG and graphite flake materials. We believe that the distinct expansion behaviour of graphite foil is a consequence of its particular morphological features and packing configuration. Specifically, the morphology of graphite foil is typically made up of disordered stacks of micrometer-sized graphitic platelets that exhibit many folds, wrinkles and voids in their structure, as noticed from field-emission scanning electron microscopy (FE-SEM) images (Fig. 1a). On the other hand, the HOPG crystals and graphite flakes are comprised of very tightly packed layers with no or very little voids in-between such layers (Fig. 1b and c). The peculiar morphology of graphite foil is a direct result of its production process, which is based on roll compaction of thermally expanded graphite particles and leads to a relatively low density product (~0.7-1.3 g cm^{-3} according to the specifications of the manufacturer, to be compared with a value of ~2.25 g cm^{-3} for HOPG). It is then reasonable to assume that the presence of a large number of

openings and gaps within the layers facilitates the intercalation of chemical species (e.g., halide anions and water molecules) in graphite foil and its subsequent expansion during the anodic treatment, whereas such a relative advantage would be essentially absent from graphites with a more compact morphology (HOPG and graphite flakes). We also note that explorative exfoliation experiments at different bias voltages, both higher and lower than 10 V, were carried out. We observed that the exfoliation process was only successful when using bias voltages above a threshold value of ~4 V, but at such low voltages the flowing current and thus the yield of exfoliated product were lower, whereas the quality of the resulting graphene flakes did not change compared to exfoliation at 10 V. For bias voltages above 10 V, neither the amount of exfoliated product nor its quality changed significantly. Concerning the current profile during exfoliation, generally speaking it was observed to increase at first, probably as a result of the expansion of the graphite anode and the ensuing increase in surface area exposed to the aqueous electrolyte. However, after some time the current tended to reach a plateau. The latter was probably due to the fact that further increases in surface area resulting from exfoliation were counteracted by the loss of expanded graphite fragments that were seen to detach from the anode.

The distinct fate of graphite foil was apparent from the FE-SEM images of the anodically treated materials, as exemplified in Fig. 1d, e, and f using 0.05 M NaCl as the electrolyte. While graphite foil (Fig. 1d) was seen to expand considerably as a result of the anodic process, yielding very thin and well separated layers, a rather limited extent of cleavage was noticed for both HOPG (Fig. 1e) and graphite flakes (Fig. 1f), which exhibited just partially detached graphite platelets of a relatively large thickness. It is thus not surprising that the subsequent mild sonication step was able to complete delamination of the anodically treated graphites into graphene flakes only for the case of graphite foil, but not for the poorly expanded HOPG and graphite flake materials. In line with this result, the effect of compact vs. loose configuration of the graphite anode has been recently highlighted by Yang et al, who reported that a modest pre-expansion of graphite foil prior to the anodic exfoliation step with a sulfate-based electrolyte brings about a considerable increase in the amount of generated single-/few-layer graphene flakes.[29] In the present case, we surmise that the intercalation and/or expansion of graphites using halide-based electrolytes are relatively inefficient processes compared to those associated to the use of

commonly employed electrolytes (e.g., sulfate-based ones). Thus, the deployment of graphite types for which the intercalation/expansion process is facilitated due to a suitable morphology (e.g., having a large amount of interlayer openings, voids and gaps) could make a critical difference in attaining a well-expanded product that can then be separated into single-/few-layer graphene flakes, as was actually observed here with graphite foil compared to HOPG and graphite flakes. Consequently, the former graphite type was used exclusively for the remainder of this work. This forced choice of graphite turns out to be quite advantageous with a view to up-scaling the graphene production process, taking into account that graphite foil is a widely available and modestly priced commodity (less than US$0.1 per gram, compared to ~US$100 per gram for HOPG). The fact that virtually no graphene can be obtained with HOPG and graphite flakes does not necessarily mean that the halide anions do not intercalate such graphites at all, but rather that if intercalation takes place, it is too slow and/or limited in extent so as not to allow an efficient exfoliation of these graphite types into graphene. Indeed, the latter are known to be readily intercalated and delaminated by other commonly used anions, such as sulfates.

The second decisive factor for successful anodic exfoliation using sodium halides was the electrolyte concentration. In general terms, for a given applied bias voltage, the anodic process is only able to afford graphene products within a certain range of electrolyte concentrations.[17] We tested the range of concentrations for each electrolyte, and found a range where the exfoliation process is effective for each sodium halide. If the electrolyte concentration is too low, the graphite anode will be poorly intercalated and no or very little expanded product will be obtained. If the concentration is too high, a very vigorous and fast intercalation process will usually take place, so that graphite fragments detach too quickly from the anode without having completed their layer-by-layer expansion. As a result, a large amount of incompletely expanded material will be attained, which cannot be subsequently separated into single-/few-layer graphene flakes via sonication, but gives rise to multilayer graphitic platelets instead, which are unstable in colloidal dispersion and appear as thick (>10 nm) objects in AFM images. However, if an intermediate electrolyte concentration is used, the process is slow enough for the detaching graphite fragments to expand and delaminate to an extent large enough so as to yield graphene nanosheets after sonication. As a result of this behavior, the final concentration of graphene dispersed in

solvents as a function of electrolyte concentration is seen to go through a maximum at intermediate electrolyte concentrations (see Table 1 and discussion below). Such a constraint in the useful concentration range was seen to be particularly stringent in the case of sodium halides. To determine the useful concentration ranges for NaCl, NaBr and NaI, pieces of graphite foil of fixed dimensions were subjected to a positive voltage (+10 V, 60 min) in aqueous solutions of the aforementioned salts at different concentrations (see Experimental section for details). The resulting expanded products (if any) were thoroughly rinsed with water and ethanol to remove remnants of salts and other reaction products, and were subsequently dispersed via sonication either in DMF or in water/FMN. This cleaning process was seen to be a vital step for the colloidal stability of the final graphene product, as very small amounts of residual salts will drastically reduce the colloidal stability of the dispersions. After a centrifugation step intended to sediment the non-fully exfoliated fraction of the material, the concentration of the supernatant, which was the final graphene dispersion, was measured using UV-vis absorption spectroscopy. We carried out a control experiment under the same conditions in the absence of any electrolyte (i.e., only in pure water), in order to test the possible influence of the hydroxide anions present in water. In this case, no change was seen in the graphite anode and no expanded material was obtained.

Table 1 shows the concentration of graphene suspensions in DMF obtained with different concentrations of the sodium halides in the anodic expansion process. The use of water/FMN as a dispersing medium instead of DMF yielded similar results. A graphene concentration value of zero indicates that no significant amount of material could be achieved in the final suspension, either because no anodically expanded product could be generated (at low electrolyte concentrations) or because virtually all the expanded product sedimented after the sonication and centrifugation steps (at high electrolyte concentrations). It can be noticed that NaCl afforded the narrowest useful range of concentrations. Indeed, dispersions of graphitic material were only attained at the tested NaCl concentration of 0.05 M, whereas concentrations of 0.1 M and above as well as 0.01 M and below failed to yield any suspended material. In the case of NaBr, the useful range was seen to be slightly broader, with significant amounts of dispersed graphitic material being obtained at electrolyte concentrations of both 0.05 and 0.1 M. Finally, NaI was determined to perform effectively as an electrolyte in a relatively broad concentration range (between 0.01 and 0.2

M), leading in all cases to very stable, homogeneous dispersions (see inset to Fig. 2 for a digital photograph of representative dispersions in water/FMN obtained with the three sodium halides). As a tentative explanation for this behaviour, we note that the reduction potential of the iodide anion is lower than that of its bromide and chloride counterparts (see below), so that the better exfoliation behavior with iodide can be ascribed to a more extensive formation of the resulting intercalated molecular species (i.e., I_2 in the case of iodide) that can therefore promote layer cleavage to a larger extent than that attained with bromide and chloride. We also note that aqueous chloride anions are not known from the literature to intercalate graphite. This could be an indication that such anions are indeed more difficult to intercalate compared to the case of bromide and iodide anions. We believe that the fact that chloride intercalation of graphite is not generally thought to be possible is due to the very narrow range of concentrations that make the intercalation (and exfoliation) possible, as well as the critical role of the type of graphite material used. As we have demonstrated here, the use of a graphite anode with many interlayer openings and voids in its structure (i.e., graphite foil) is critical to make intercalation and exfoliation possible. This result suggests that intercalation of chloride anions into graphite is possible provided that it is facilitated through the use of graphites with somewhat increased interlayer spacings. Consequently, we do not believe that the mechanism of chloride intercalation is fundamentally different to that bromide, iodide or other electrolytes; it only needs larger graphite interlayer spacings to proceed.

The graphitic nature of the suspended material was made apparent by UV-vis absorption spectroscopy, as demonstrated in Fig. 2 for dispersions in water/FMN solutions. The spectra were dominated by an absorption peak located at ~265-270 nm together with strong absorbance in the whole wavelength range above 270 nm. These features are characteristic of sp^2-based carbon systems having extended electronically conjugated domains and have been observed, e.g., both on pristine graphene and on well-reduced graphene oxide nanosheets.[35] The very weak, shoulder-like absorption bands noticed at about 250, 375 and 450 nm correspond to absorbance from the FMN stabilizer.[34] As evaluated by this technique, significant amounts of suspended graphitic material (up to ~0.75 mg mL^{-1}) were attained for the as-prepared suspensions following the protocol described in the Experimental section. However, they could be further increased to the

range of several milligrams per milliliter through different post-processing concentration strategies, including partial solvent removal using a rotary evaporator or sedimentation of the suspension via high-speed centrifugation and re-dispersion in a smaller solvent volume.[34] The energy consumption in the anodic exfoliation process is largely due to the current flowing through the cell, and is estimated to be ~0.05 kW h for a usual experiment carried out in our laboratory considering the power consumption of the power supply.

2.2. Characteristics of the exfoliated products and role of the halide anions in the exfoliation process

Having demonstrated that sodium halides can indeed be used in aqueous anodic exfoliation processes to give stable dispersions of graphitic materials, the next step of the investigation focused on determining their physicochemical characteristics. First, the lateral size and exfoliation degree of the dispersed graphitic materials were investigated by means of scanning transmission electron microscopy (STEM) and atomic force microscopy (AFM). Fig. 3 shows typical STEM (a,b,c) and AFM (d,e,f) images recorded from water/FMN dispersions obtained with the three different electrolytes at a given concentration within their respective useful ranges: 0.05 M NaCl (a,d), 0.1 M NaBr (b,e) and 0.1 M NaI (c,f). All the dispersions were comprised of thin nanosheets with mean lateral dimensions of 560±210, 655±390 and 610±260 nm for 0.05 M NaCl, 0.1 M NaBr and 0.1 M NaI respectively, and apparent thickness (derived from AFM height profiles) between ~2 and 3 nm. The apparent thickness values for nanosheets from dispersions obtained at other sodium halide concentrations were very similar and are given in Table 1. The lateral size of the graphene flakes is mainly limited by the sonication step applied to the electrolytically expanded graphite material and it is in the same range as that measured for other electrolytes we have reported before. We also note that in the present work we searched for conditions that allow an efficient delamination of the graphite anode so as to attain very thin graphene nanosheets. In addition to the electrolytic treatment, sonication and centrifugation steps were applied to the electrochemically delaminated material. The main role of these steps, particularly centrifugation, is to select very thin nanosheets generated in the process (if any are generated at all). Therefore, it is not surprising that we obtained similar thickness values for all the samples, because the applied processes were

indeed meant to select the thinnest nanosheets. The fact that different halides lead to different amounts of nanosheets ~~was~~ is most probably a result of the different efficiency of the electrolytes in the delamination of the graphite anode. Considering that AFM thickness measurements of graphene nanosheets on SiO_2/Si and other substrates are affected by a positive offset of ~0.5-1 nm[36] and that FMN molecules adsorbed on both sides of the nanosheets could also contribute to the measured thickness, we conclude the actual thickness of these nanosheets to be not larger than ~0.5-1.5 nm, implying that they are typically comprised between one and four monolayers. Such a result indicates that a high degree of exfoliation could be attained with these electrolytes. For electrolyte concentrations above the useful range, virtually no suspended graphitic material was attained after the sonication and centrifugation steps, as noted above. However, AFM inspection of a sonicated suspension that was allowed to stand undisturbed overnight (no centrifugation) revealed that it was comprised of relatively thick objects (typical apparent thickness above ~10 nm). This observation corroborated the idea that high electrolyte concentrations lead to an inefficient exfoliation of the graphite anode.

Chemical analysis of the dispersed materials was carried out by X-ray photoelectron spectroscopy (XPS). Fig. 4 shows survey spectra (a,c,e) as well as high resolution C 1s core level spectra (b,d,f) for graphene dispersions obtained with 0.05 M NaCl (a,b), 0.1 M NaBr (c,d) and 0.1 M NaI (e,f). In all cases carbon was the dominant element, although oxygen was also present to a significant but variable extent depending on the specific electrolyte concentration used for exfoliation. Signals corresponding to the halogen used in the anodic process were not observed, i.e., the amount of halogen present in the graphene samples was below the detection limit of this technique (~0.1 at%), implying that the washing procedure applied to the anodically expanded products was rather effective. This is an advantage over some previously reported electrolytes that cannot be readily removed due to their strong adsorption onto the graphene nanosheets.[30] Another advantage of the present electrolytes is related to their cost: sodium halides are simple, inexpensive and widely available chemicals. The O/C atomic ratios for the different tested electrolyte concentrations are given in Table 1, which were seen to range between 0.06 and 0.11. The high resolution C 1s spectra provided information on the nature of the oxidized carbon species. These spectra comprised a majority component located at ~284.6 eV that could be ascribed to carbon

atoms in unoxidized graphitic environments (C=C species) and a minor component at about 286.7 eV, which was attributed to carbon atoms single-bonded to oxygen (C-O species), for example in hydroxyl, ether or epoxy groups.[24] The XPS results thus indicated that the exfoliated graphene nanosheets were oxidized only to a limited extent. Specifically, the O/C atomic ratio of samples prepared with 0.05 M NaCl (0.06) and 0.1 M NaBr (0.07) lay at the lower end of the range of values that have been reported for most graphenes anodically exfoliated using a number of inorganic or organic electrolytes, such as sulfuric acid (O/C ratios ~0.08-0.3),[17,18,22,30,37] sulfate salts (~0.06-0.19),[17,18,22,30,38] phosphoric acid (~0.3),[23] lithium perchlorate (~0.25),[22] sodium methanesulfonate (~0.15)[39] or sodium citrate (~0.13).[25]

To understand the origin of the limited oxidation degree of the graphene nanosheets exfoliated here with the sodium halides, the possible redox processes involving these electrolytes and the evolution of oxygen species as a result of water oxidation at the graphite anode must be considered. First of all, as outlined above, it is believed that anionic intercalation in general strongly relies on the oxidation of edges and defects of the graphite anode by water molecules from the aqueous electrolyte. This oxidation induces a significant increase in the interlayer spacing of graphite in the local area around the edges. In turn, such a local increase in the interlayer spacing allows even relatively large anions to penetrate the graphitic material at the edges, which thus act as a wedge facilitating the subsequent separation of the graphite layers at regions increasingly farther from the edges. On the basis of this general mechanism, it follows that having a graphite anode with many pre-existing interlayer voids and openings, as it is the case with graphite foil, should clearly facilitate the intercalation and exfoliation of the anode, especially in cases where anion intercalation appears to be generally difficult (e.g., the present halides). Second, we note that halide intercalation in the interlayer spaces at the positively biased graphite electrode should take place most likely in the form of hydrated anions, i.e., halide anions surrounded by a bound shell of water molecules[40,41,42] (see step A in the schematic process chart of Fig. 5). At the high anodic potential used (10 V), oxygen evolution reactions take place and these water molecules are expected to readily oxidize (step B1 in Fig. 5), giving first hydroxyl radicals (·OH) and then oxygen molecules (O_2) through further oxidation[43] (step C1). The build-up of gaseous O_2 in the interlayer spaces should exert a considerable

pressure on the graphitic layers and hence contribute to their separation from one another. Additionally, some of the generated ·OH radicals can attack the exfoliated layers (step C2), so that the resulting graphene nanosheets will bear a certain degree of oxidation. Third, it is reasonable to assume that the intercalated halide anion itself also participates in redox processes. In particular, it can be oxidized at the graphite electrode (step B2) to give the corresponding diatomic molecule (e.g., I_2 will be obtained from the anodic oxidation of I^-). As a matter of fact, when using NaBr and NaI as the electrolyte we observed that the aqueous solution progressively turned brown or red-brown around the graphite anode, such a color being characteristic of Br_2 and I_2 dissolved in water. For NaCl no color change was observed: Cl_2 is readily hydrolyzed to give colorless HCl and HClO (or their corresponding sodium salt forms). In any case, accumulation of the halide oxidation products in the interlayer spaces should also contribute to separate the graphene sheets and therefore to the overall exfoliation process, in a similar way as it has reported to happen when using sulfate salts for the same process.[17]

However, besides reacting directly with the graphite anode, the halide anions can also be oxidized by the generated ·OH radicals (step C3 in Fig. 5). This reaction is thermodynamically feasible for the three halides contemplated here. Indeed, the standard reduction potential of the different halogen/halide pairs in aqueous solution are +1.37 V for Cl_2/Cl^-, +1.09 V for Br_2/Br^- and +0.54 V for I_2/I^-,[44] compared with a value of +1.9 V for the $\cdot OH/OH^-$ pair.43 Furthermore, the oxidation of aqueous Cl^-, Br^- and I^- ions by ·OH radicals has been well investigated in the past,[45,46,47] and such a process is known to involve conversion of the highly oxidizing ·OH radicals to hydroxide anions (OH^-) or water molecules. The reaction of ·OH radicals with halide anions would thus be expected to prevent, at least to some extent, the attack of the graphite electrode by the former species, thus providing a mechanism to mitigate the oxidation of the graphene nanosheets that result from the anodic treatment. On the other hand, this type of reaction is not expected to occur when the electrolyte is comprised of a non-oxidizable anion, such as the sulfate, perchlorate or phosphate anion (for these anions, S, Cl and P are in their corresponding highest possible oxidation state). Hence, under such circumstances the intercalating anions would not be able to curtail the oxidation of the graphene lattice. Based on these considerations, we conclude that the halide anions play a dual role in the anodic exfoliation of graphite to give

graphene nanosheets: (1) they act as intercalating electrolyte to promote the exfoliation of graphite, and (2) they mitigate the oxidation of the exfoliated graphene nanosheets by acting as scavengers of the highly reactive oxygen radicals generated during the anodic process. We also note that the presence of voids and openings in the starting graphite foil electrode could contribute to mitigate the oxidation of the resulting graphene nanosheets, as it is expected to make the exfoliation process faster and less reliant on the oxidative opening of the interlayer spaces compared with the use of more compact types of graphite (e.g., graphite rods).[18,33]

In addition to the morphological and chemical analysis, the structural quality of the anodically exfoliated graphenes was probed by Raman spectroscopy, as illustrated in Fig. 6 for samples prepared with 0.05 M NaCl (a), 0.1 M NaBr (b) and 0.1 M NaI (c). In all cases, the well-known G and D bands associated to graphite/graphene-based materials and located at about 1582 and 1350 cm^{-1}, respectively, were seen to dominate the first-order region of the spectra (i.e., the 1100–1700 cm^{-1} region), whereas the main feature observed in the second-order region (2300–3300 cm^{-1}) was the so-called G´ or 2D band (~2700 cm^{-1}). As noticed from Table 1, the integrated intensity ratio of the D and G bands (I_D/I_G ratio), which is usually taken as a quantitative measure of the structural disorder present in graphite/graphene materials,[48] was seen to differ somewhat between the different graphene samples. Indeed, the I_D/I_G ratio tended to positively correlate with the O/C atomic ratio. Such a result was reasonable considering that anodic oxidation of the graphene nanosheets should be associated to the covalent grafting of oxygen functional groups on the carbon lattice (e.g., hydroxyl groups; see XPS results from Fig. 4), which in turn should convert a fraction of the originally sp^2-hybridized carbon atoms to defect-like sp^3-hybridized species. We note that, in the calculation of the I_G value (integrated intensity of the G band), we explicitly exclude the contribution of the D´ band, which appears as a shoulder on the high wavenumber side of the G band (~1620 cm-1). Because we are calculating the I_D/I_G ratio and not the $I_D/(I_G+I_{D'})$ ratio, we first have to determine the areas associated to the G and D´ bands through a peak-fitting procedure. This implies that the actual area of the G band is obviously smaller than the area of the composite (G+D´) envelope. As a result, the I_D/I_G ratios given in Table 1 might appear to be somewhat larger than the values an observer would guess through direct visual inspection of the spectra shown in Fig. 6. We also

measured the electrical conductivity of free-standing, paper-like graphene films obtained through vacuum filtration of the corresponding dispersions in water/FMN. For example, the conductivities of films made up of nanosheets obtained via exfoliation in 0.1 M NaBr (~10 μm thick, as determined by FE-SEM) and 0.1 M NaI (~12 μm thick) were 15220 and 6750 S m^{-1}, respectively. These values were lower by a factor of ~3-6 than those previously reported for films derived from completely defect-free, pristine graphene flakes produced by direct ultrasound-induced exfoliation of graphite in water/FMN solutions,[34] which can be attributed to the somewhat defected nature of the present anodically exfoliated materials. On the other hand, they were similar to the conductivity values measured beforehand for films made up of pristine graphene flakes prepared by ultrasound-exfoliation in water with such stabilizers as sodium dodecylbenzenesulfonate (~1500 S m^{-1}),[49] sodium cholate (~15000 S m^{-1}),[50] sodium taurodeoxycholate (~13000 S m^{-1})[51] or gum Arabic (~10000 S m^{-1})[52]. We note that these prior values could only be obtained after removing at least part of the stabilizer from the as-filtered films through an appropriate treatment (e.g., high temperature annealing under inert or reducing atmosphere), whereas no post-treatment of the films was required in the present case to achieve similar conductivity results.

2.3. Use of halide-based anodically exfoliated graphene in energy- and environment-related applications

Owing to their high surface area, good electrical conductivity as well as prominent chemical, mechanical and thermal stability, graphene materials are widely investigated towards their implementation in a number of environment- and energy-related applications, including their use as sorbents for oils and water-soluble organic compounds (e.g., dyes),[53] or as electrodes for supercapacitors and Li-ion batteries.[54] Central to a successful performance in many of these applications is the ability to assemble the graphene sheets into three-dimensional, macroscopic and porous structures in which the accessible area of each individual sheet is retained to the largest possible extent. This has been typically accomplished via appropriate processing of graphene oxide nanosheets or through CVD protocols that make use of metal foams as templates,[55] but such strategies are generally time-consuming, elaborate and/or costly. As an alternative that could be competitive in terms of both performance and cost, we propose to use the as-exfoliated graphene materials

developed here for some of the mentioned applications. Before their dispersion in any solvent via sonication, these materials exhibit a foam-like appearance (Fig. 7a), with an estimated density of ~40-45 mg cm^{-3}, and are comprised of expanded and loosely connected graphene layers having micrometer- to nanometer-sized gaps in-between (Fig. 1d and inset to Fig. 7a). The extremely simple and expeditious nature of their preparation process (just anodic treatment of graphite foil in sodium halide electrolyte) could facilitate the large-scale deployment of such graphene products in many practical uses. Thus, to probe their potential, we examined their performance as adsorbents for dyes and non-polar organic solvents/oils, as well as electrodes for supercapacitors. The material exfoliated in 0.1 M NaI was selected for these studies mainly because it affords the largest amount of graphene products among all the tested electrolytes (see Table 1), which is advantageous from the viewpoint of applications.

Fig. 7b shows the adsorption capacity of the as-exfoliated graphene product towards several dyes in aqueous solution, namely, rhodamine B, basic fuchsin, methylene blue and methyl orange, measured at room temperature (295 K) and pH ~6. For the three cationic dyes (i.e., rhodamine B, basic fuchsin and methylene blue), values between 300 and 400 mg g^{-1} were obtained, being comparable to or even higher than those of many graphene-based adsorbent materials that have been previously reported.[7,53,56,57,58] In most prior work, however, the adsorbents typically comprised graphene oxide or reduced graphene oxide nanosheets, which favored adsorption through electrostatic attraction between the positively charged dyes and the negatively charged (ionizable) oxygen functional groups present in the nanosheets (e.g., carboxylates), with π-π stacking probably also playing some role.[53,57] On the other hand, although an electrostatic component could certainly be in place for the present anodically exfoliated materials by virtue of their non-negligible oxidation, we believe dye adsorption to be more reliant on π-π interactions in this case. This is because anodically exfoliated graphenes tend to possess a more graphitic (electronically conjugated) character than that of graphene oxides/reduced graphene oxides with a similar or even smaller extent of oxidation.[59] Furthermore, the adsorption capacity measured for the anionic dye methyl orange was substantially higher than that of its cationic counterparts (~920 mg g^{-1}), a result that is not consistent with a predominance of negatively charged adsorption sites on the graphene sheets. To the best of our knowledge, the adsorbed amount

of methyl orange was the highest ever reported for a graphene-based adsorbent. The different adsorption performance of the anodically exfoliated material towards methyl orange and the three other dyes is currently not understood, but we hypothesize that it is related to differences in packing densities of the molecules on the graphene surface. A comparison of dye adsorption capacities of different graphene-based materials from the literature is provided in Table S1 of the Electronic Supplementary Information. Likewise, due to its primarily hydrophobic nature, the anodically exfoliated material was a good sorbent for non-polar organic solvents and oils, such as toluene, hexane, dodecane, tetrahydrofuran, acetone, chloroform, ethylenglycol, ethanol, olive oil or pump oil, with the measured sorption capacities ranging between ~12 and 24 g g^{-1} (Fig. 7c). Although such values are lower than those of lighter graphene and other carbon-based sorbents reported in the literature (e.g., lightweight graphene aerogels), they are comparable to those of sorbents with a similar density.[7,56,60] Nonetheless, we expect that the oil sorption performance of the anodically exfoliated materials can be significantly improved on the basis of simple strategies, such as working with starting graphite foils of a lower density (densities down to ~0.05 g cm^{-3} have been reported, compared to a value of 0.7-1.3 g cm^{-3} for the foils used here). Because the use of a graphene or any other material in environmental applications could require such material to be non-cytotoxic, we also explored the biocompatibility of the present graphenes. In particular, we investigated the proliferation of murine fibroblasts onto halide-based graphene film substrates. The results (see SI) suggested these materials to be biocompatible.

Finally, the as-exfoliated graphene material was explored as a supercapacitor electrode in aqueous 1 M H_2SO_4 electrolyte (two-electrode configuration). The recorded cyclic voltammetry (CV) curves (Fig. 8a) exhibited an almost rectangular shape with negligible deviation at the limit potentials, even for a voltage window as wide as 1.4 V (CV curves were also obtained in a three-electrode configuration, and are presented and discussed in the Electronic Supplementary Information). This rather unusual, wide operation voltage was further confirmed by charging-discharging the supercapacitor cell at 0.1 A g^{-1}. As noticed from Fig. 8b, the galvanostatic charge-discharge profiles kept a triangular form when the voltage was gradually increased from 1.1 to 1.4 V. We note that the working voltage window of two-electrode symmetric cells using aqueous electrolytes is generally

limited by the electrolytic decomposition of water to values ~1 V.[61] In particular, a voltage window of 1.4 V is considerably larger than that usually observed for porous carbon-based aqueous supercapacitors. For conventional porous carbons (e.g., activated carbons), although physisorption can furnish the water molecules with some degree of stability against electrolytic decomposition, the extensive presence of amorphous and/or highly defective structures in their lattice, which act as reactive chemisorption sites, tends to promote water electrolysis. On the other hand, such reactive sites are expected to be much less abundant in the as-exfoliated graphene materials investigated here due to their well-preserved graphitic character (Fig. 6). This feature, together with the particular morphology of voids and pores observed for this material (inset to Fig. 7a), is believed to contribute to a broader voltage window.

The evolution of electrode performance with current density was also investigated on the basis of charge-discharge tests at 1.4 V, and the results were used for the construction of the Ragone plot shown in Fig. 8c. Even though the cells yielded modest values of specific capacitance (e.g., 50 F g^{-1} at 0.1 A g^{-1}), the fact that the device could be operated at a relatively high voltage led to remarkable energy and power density characteristics, with values up to 15.3 Wh kg^{-1} and 3220 W kg^{-1}, respectively. Such a good capacitive behavior was made apparent by comparison to other similar graphene-based materials that have been previously reported (also given in Fig. 8c). For example, the power and energy densities delivered by the present graphene material were comparable or even higher than those of many three-dimensional graphene structures (such as graphene aerogels),[62,63,64,65,66] graphene films,[67] graphene compounded with electroactive materials (e.g., polyaniline),[68] or graphene/porous carbon hybrids.[69,70] It is important to note that in addition to competitive performance, a critical advantage of the present graphene materials lies in the extreme simplicity and environmental friendliness of their preparation compared with that of other graphene materials that rely on harsh chemical treatments (e.g, those based on graphene oxide), high temperatures and/or complex processing strategies (e.g., supercritical or freeze drying). Additional evidence of the cell stability was demonstrated on the basis of cycling tests (Fig. 8d), which revealed that ~98% of the initial capacitance was retained after 5000 cycles at 1 A g^{-1}. The plots in Fig. 8d suggest a significant internal resistance (IR) drop in the cell, which is discussed in the Supporting Information. In any case, we

believe that the approach described here could greatly facilitate the practical implementation of graphene materials towards supercapacitor applications.

3. Conclusions

We have demonstrated that sodium halides (NaCl, NaBr and NaI) are efficient electrolytes in the aqueous anodic exfoliation of graphite, affording single-/few-layer graphene nanosheets of a high structural quality and limited oxygen content. The successful role of these salts as exfoliating electrolytes was seen to rely on two key aspects. First, a proper selection of the graphite source material was required, in particular graphites having many openings, gaps and inner voids in their structure. In this regard, graphite foil (a modestly priced commodity) turned out to be an appropriate choice. Second, identification of an operative range of salt concentrations was also critical towards successful exfoliation. Such a range was seen to be particularly tight in the case of NaCl and NaBr. In addition to their role as exfoliating electrolyte, the halide anions were concluded to act as sacrificial agents that prevented the extensive oxidation of the graphene lattice during anodic exfoliation. Such an oxidation-preventing ability was ascribed to the relatively low redox potentials of these anions. Significantly, the as-exfoliated graphene materials exhibited a three-dimensional morphology that allowed their direct use in a number of energy- and environment-related applications, thus avoiding the complex processing steps that are usually required for many graphene-based materials. Testing of the halide-derived graphene products as dye adsorbents, as sorbents for oils and non-polar organic solvents, and as electrodes for supercapacitors revealed a performance comparable to or even higher than that frequently reported for different types of graphene (e.g., those obtained from graphite oxide). Cell proliferation tests also indicated a good biocompatibility of the halide-derived graphenes. Overall, we believe that the extremely simple and environmentally friendly nature of the production/processing method of graphene described here, combined with a competitive performance of the material in some relevant applications, constitutes a significant step forward towards the practical implementation of graphene in many real-life applications. Further efforts to improve the performance of the graphene materials in these and other applications along the lines proposed in this work are currently under way.

4. Experimental

4.1. Materials and reagents

Graphite anodes used throughout the study consisted of high purity graphite foil (Papyex I980, acquired from Mersen). For comparison purposes, highly oriented pyrolytic graphite (HOPG; grade ZYH, obtained from Advanced Ceramics) and natural graphite flakes (Sigma-Aldrich, ref. 332461) were also employed. NaCl, NaBr and NaI solutions in Milli-Q water were used as electrolytes. N,N-dimethylformamide (DMF) was used as a dispersing solvent for graphene, and flavin mononucleotide (FMN, riboflavin 5′-monophosphate sodium salt) was used as a stabilizer to colloidally disperse the graphene flakes in aqueous medium. All these chemicals were purchased from Sigma-Aldrich and used as received.

4.2. Aqueous anodic exfoliation of graphite using sodium halides as the electrolyte

The anodic exfoliation process was carried out in a two-electrode configuration, using a piece of graphite foil (dimensions: 40×25×0.5 mm^3) as the anode and a platinum foil (dimensions: 25×25×0.025 mm^3) as the cathode. HOPG pieces and graphite flake pellets were also used as anodes. In all cases both anode and cathode were held by spring clips connected to the current source. Both electrodes were immersed in an aqueous solution (20 mL) of a sodium halide (NaCl, NaBr or NaI) at a certain concentration (specified below). A positive voltage (10 V) was then applied to the graphite anode for 60 min using an Agilent 6614C DC power supply. The platinum foil cathode was placed parallel to the graphite foil surface at a distance of about 2 cm. During this process, gas bubbles formed in both electrodes, with the graphite anode being typically seen to expand and release graphitic fragments from its surface. After the 60 min electrolysis period, the resulting expanded graphitic product was gently rubbed off from the graphite anode using a spatula, thoroughly rinsed with copious amounts of Milli-Q water and ethanol to remove residual salts as well as other products of the electrochemical reaction and then dried overnight at room temperature under reduced pressure. Subsequently, this expanded material was sonicated in a given volume (20 mL) of either DMF or aqueous FMN solution (1 mg mL^{-1}) for 3 hours (Selecta Ultrasons system, 40 kHz), and then the resulting dispersion was centrifuged at

200 g for 20 min (Eppendorf 5424 microcentrifuge) to sediment insufficiently exfoliated material. The obtained supernatant was collected and stored for further use. In the case of the FMN-stabilized aqueous dispersions, they were further purified (to remove the fraction of free, non-adsorbed FMN from the medium) by two cycles of sedimentation via centrifugation (20000 g, 20 min) and re-suspension in Milli-Q water with a brief sonication step.

4.3. Characterization techniques

Characterization of the graphene samples was carried out by means of UV-vis absorption spectroscopy, Raman spectroscopy, X-ray photoelectron spectroscopy (XPS), field emission scanning electron microscopy (FE-SEM), scanning transmission electron microscopy (STEM), atomic force microscopy (AFM) and measurement of electrical conductivity. UV-vis absorption spectroscopy was carried out with a double-bean Heλios α spectrophotometer, from Thermo Spectronic. Following previous reports,[18,34] the suspension concentration was estimated by means of UV-vis absorption spectroscopy on the basis of the Lambert-Beer law and using a value of 2440 mL mg^{-1} m^{-1} for the extinction coefficient at the measured wavelength of 660 nm. Raman spectra were acquired with a Horiba Jobin-Yvon LabRam instrument at an incident power of 2.5 mW and using a laser excitation wavelength of 532 nm. XPS measurements were performed on a SPECS apparatus at a pressure of 10^{-7} Pa and using a non-monochromatic Mg K_α X-ray source (11.81 kV, 100 W). Samples for both Raman spectroscopy and XPS were prepared by drop-casting the corresponding aqueous, FMN-stabilized graphene dispersion onto a pre-heated (~50-60 ºC) circular stainless steel sample-holder 12 mm in diameter to give thin, macroscopic graphene films. XPS survey spectra were used to determine the overall elemental composition of the graphene samples in such films. Although XPS is a surface-sensitive technique that only probes the outermost surface layer of materials (a few to several nanometers deep), in the case of graphene samples prepared from colloidal dispersions it can be inferred that the elemental compositions derived from XPS are representative of the whole sample. Because the colloidal graphene suspensions used to prepare the thin films are expected to be spatially homogeneous, there is no reason to believe that the graphene nanosheets constituting the other surface of the formed films are

not representative of the whole graphene sample, i.e., the graphene sheets probed in the XPS measurement must be representative of the sample as a whole. Also, because the thickness of the graphene nanosheets is generally comparable to the probing depth of XPS, this technique must probe individual graphene nanosheets in its entirety, and not just the outer surface of nanosheets. Having these two factors in mind, we have to conclude that survey XPS spectra must provide a reasonably accurate picture of the elemental composition of this type of graphene samples. FE-SEM and STEM imaging was accomplished with a Quanta FEG 650 system (FEI Company) operated at 20-30 kV. Specimens for STEM were prepared by mixing a given volume of aqueous graphene suspension with an equal volume of ethanol, and then 40 μL of the resulting water-ethanol dispersion were drop-cast onto copper grids (200 mesh) covered with a thin continuous film of amorphous carbon. AFM images were recorded on a Nanoscope IIIa Multimode apparatus (Veeco Instruments) in the tapping mode of operation under ambient conditions. Rectangular silicon cantilevers with nominal spring constant and resonance frequency values of ~40 N m^{-1} and 250-300 kHz, respectively, were employed. HOPG pieces or SiO_2(300 nm)/Si wafers were used as substrates in the preparation of specimens for AFM. To this end, a small volume (20-40 μL) of the graphene dispersion at a concentration of ~0.05 mg mL^{-1} was drop-cast onto the HOPG or SiO_2/Si substrate pre-heated at ~50-60 ºC and then allowed to dry. For the measurement of electrical conductivity, free-standing paper-like films were prepared from the aqueous graphene dispersions by vacuum filtration through silver membrane filters 25 mm in diameter and 0.2 μm in pore size (Sterlitech Corporation). Conductivity was determined through the van der Pauw method by means of a homemade setup (Agilent 6614C potentiostat and Fluke 45 digital multimeter) with 12×12 mm^2 square pieces that were cut from the free-standing films. The thickness of the films was estimated by FE-SEM.

4.4. Testing of as-prepared anodically exfoliated graphene in energy and environmental applications

The graphene material obtained by anodic exfoliation in 0.1 M NaI was tested as an adsorbent for water-soluble dyes as well as for non-polar organic solvents and oils, and as an electrode for supercapacitors. To this end, the as-exfoliated product, i.e. the material

directly generated by the anodic treatment without subsequent sonication (only washed to remove remnants of the electrolyte), was used. For the dye adsorption experiments, ~10 mg of the graphene material was added to 10 mL of an aqueous solution of the dye (rhodamine B, basic fuchsin, methylene blue and methyl orange) at room temperature and pH ~6, which was then gently stirred with a magnetic bar for 48 h to ensure that the adsorption equilibrium was attained. After removal of the graphene component via centrifugation (10000 *g*, 10 min), the concentration of dye remaining in the aqueous solution was determined through UV-vis absorption spectroscopy on the basis of absorption peaks characteristic of each dye (located at ~555 nm for rhodamine B, 540 nm for basic fuchsin, 660 nm for methylene blue and 460 nm for methyl orange), which in turn was used to infer the amount of dye adsorbed on the graphene sample. To estimate maximum adsorption capacities, different starting concentrations of the dye were probed (typically up to 1-2 mg mL^{-1}). For the oil/non-polar organic solvent sorption experiments, a certain amount of the graphene material (~5 mg) was placed in a 1.5 mL centrifuge tube, and then small known volumes of the oil/organic solvent (typically ~80-140 μL) were added in succession. These volumes were quickly absorbed by the graphene sample until a saturation point was reached, which was used to estimate the amount retained by the graphene sorbent. Sorption assays were carried out with the following compounds: toluene, hexane, dodecane, tetrahydrofuran, acetone, chloroform, ethylenglycol, ethanol, olive oil, new and used pump oil.

For the supercapacitor electrode tests, the as-exfoliated graphene material was hand-ground to obtain a homogeneous powder that was subsequently mixed with polytetrafluoroethylene (PTFE) in absolute ethanol to obtain a carbon paste (graphene:PTFE weight ratio of 8:1). This paste (~7 mg) was pressed in a mould under 1 ton for 15 s to obtain two circular pellets (~0.78 cm^2) with similar mass and thickness. The pellets were degassed at 100 ºC under vacuum for 4h, soaked into the electrolyte (1 M H_2SO_4) for 24 h, and then used as symmetric working electrodes in a two-electrode Swagelok-type with glass microfiber filter (grade 934-AH, from Whatman) acting as the separator. The supercapacitor performance was tested by means of a computer-controlled potentiostat (PGZ 402 Voltalab, from Radiometer Analytical). Cyclic voltammetry (CV) tests were performed at 10 mV s^{-1} and different voltage windows. Galvanostatic charge-

discharge profiles were recorded up to different voltages (1.1-1.4 V) and at different current loads (0.1-6 A g^{-1}). Long-term stability tests were carried out by cycling the cell at a constant current density of 1 A g^{-1} for 5000 cycles. The gravimetric capacitance, C_S (F g^{-1}) of a single electrode was calculated on the basis of the following formula:

$$C_S = \frac{2\, I\ \Delta t_d}{m\, \Delta V_d} \quad (1)$$

, where I is the current (A), Δt_d is the time of discharge at the fixed potential window (s), m is the mass of the active material within the working electrode (g) and ΔV_d is the potential difference (V) between start and finish of the discharge process after omitting the internal resistance (IR) drop. The gravimetric energy density of the electrode, E (Wh kg^{-1}), was calculated through the formula:

$$E = \frac{1}{2} C_{CELL} \Delta V_d{}^2 \quad (2)$$

, where C_{CELL} is the gravimetric capacitance of the total cell (F g^{-1}). Finally, the gravimetric power density, P (W kg^{-1}), was calculated by applying the following equation:

$$P = \frac{E}{\Delta t_d} \quad (3)$$

Supporting Information

Cell proliferation tests of murine fibroblasts grown onto halide-based graphene substrates. Characterization of as-exfoliated graphene material by N_2 physisorption. Additional XPS data of the exfoliated graphenes. Three electrode characterization of as-prepared anodically exfoliated graphene. Discussion of IR drop contribution to the supercapacitor cell performance. Table comparing adsorption capacities of dyes with different graphene-based materials.

Corresponding Author

*Telephone: (+34) 985 11 90 90. Fax: (+34) 985 29 76 62. Email: j.munuera@incar.csic.es.

Acknowledgements

Financial support from both the Spanish Ministerio de Economía y Competitividad (MINECO) and the European Regional Development Fund (ERDF) through grant MAT2015-69844-R is gratefully acknowledged. We also acknowledge partial funding by both Plan de Ciencia, Tecnología e Innovación 2013-2017 del Principado de Asturias and the ERDF through Project GRUPIN14-056. This work was also partially funded by project "AIProcMat@N2020 - Advanced Industrial Processes and Materials for a Sustainable Northern Region of Portugal 2020" (NORTE-01-0145-FEDER-000006), supported by Norte Portugal Regional Operational Programme (NORTE 2020), under the Portugal 2020 Partnership Agreement, through the European Regional Development Fund (ERDF) and of Project POCI-01-0145-FEDER-006984 – Associate Laboratory LSRE-LCM funded by ERDF through COMPETE2020 - Programa Operacional Competitividade e Internacionalização (POCI) – and by national funds through FCT - Fundação para a Ciência e a Tecnologia. A.P. thanks her research contract partially supported (80%) by the ERDF/FEDER Operative Programme of the Region of Murcia (Project No. 14-20-01). J.M.M. is grateful to the Spanish Ministerio de Educación, Cultura y Deporte (MECD) for his pre-doctoral contract (FPU14/00792).

Table 1. Characteristics of the graphene materials obtained by aqueous anodic exfoliation of graphite foil in different concentrations of the sodium halides NaCl, NaBr and NaI. [X^-]: electrolyte concentration in the aqueous anodic system. [Graphene]: concentration of graphene dispersed in DMF after anodic exfoliation, sonication and centrifugation. O/C atomic ratio derived from XPS survey spectra of the samples. Apparent thickness of the nanosheets derived from AFM height data.

Electrolyte	[X^-] (M)	[Graphene] (mg/mL)	O/C ratio	I_D/I_G	Apparent thickness (nm)
NaCl	0.01	0	-	-	-
	0.05	0.21	0.06	0.8	2-3
	0.10	0	-	-	-
	0.20	0	-	-	-
	0.50	0	-	-	-
	1.00	0	-	-	-
NaBr	0.01	0	-	-	-
	0.05	0.05	0.08	0.9	2-3
	0.10	0.26	0.07	1.1	2-3
	0.20	0	-	-	-
NaI	0.01	0.11	0.08	1.3	2-3
	0.05	0.57	0.11	1.4	2-3
	0.10	0.75	0.11	1.4	2-3
	0.20	0.24	0.08	1.2	2-3
	0.50	0	-	-	-

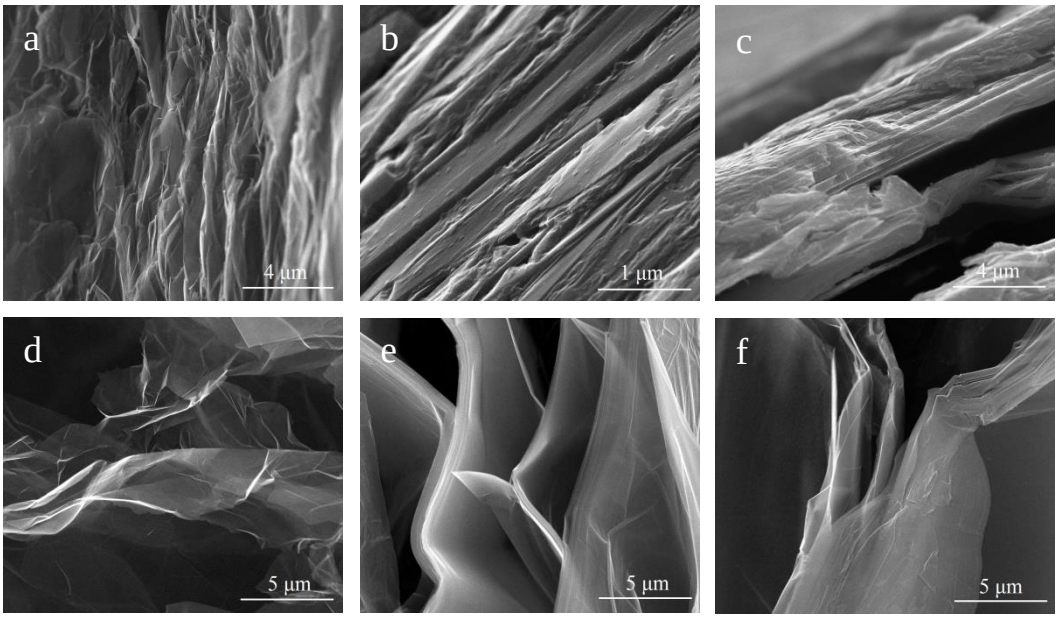

Figure 1. Representative FE-SEM images of graphite foil (a,d), HOPG (b,e) and graphite flakes (c,f) before (a,b,c) and after (d,e, f) electrochemical treatment in 0.05 M NaCl (+10 V, 60 min).

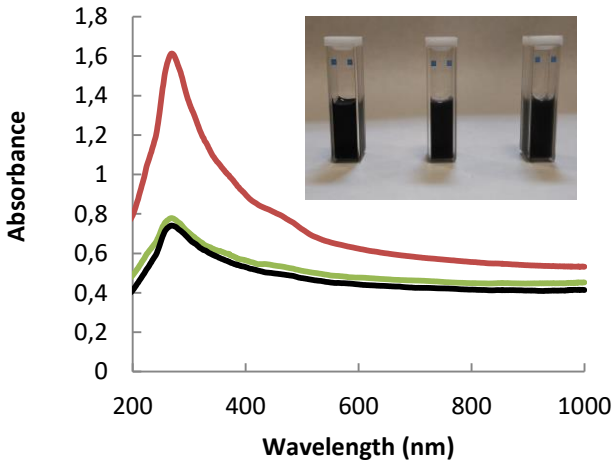

Figure 2. UV-visible absorption spectra of aqueous FMN-stabilized graphene dispersions prepared through anodic exfoliation in 0.05 M NaCl (black trace), 0.1 M NaBr (green trace) and 0.1 M NaI (red trace). Inset: digital photograph of aqueous FMN-stabilized graphene dispersions prepared with 0.05 M NaCl (right), 0.1 M NaBr (middle) and 0.1 M NaI (left).

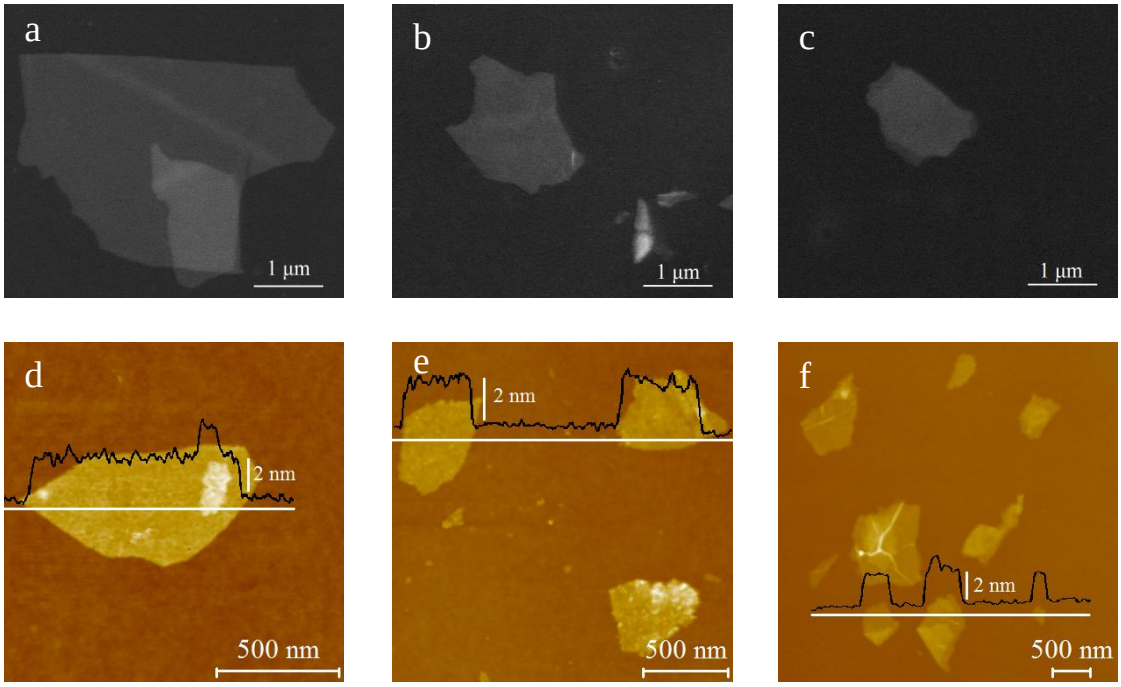

Figure 3. Representative STEM (a,b,c) and AFM (d,e,f) images of graphene nanosheets obtained by aqueous anodic exfoliation of graphite foil in 0.05 M NaCl (a,d), 0.1 M NaBr (b,e) and 0.1 M NaI (c,f). In d, e and f, line profiles (black traces) taken along the marked white lines are shown overlaid on the AFM images.

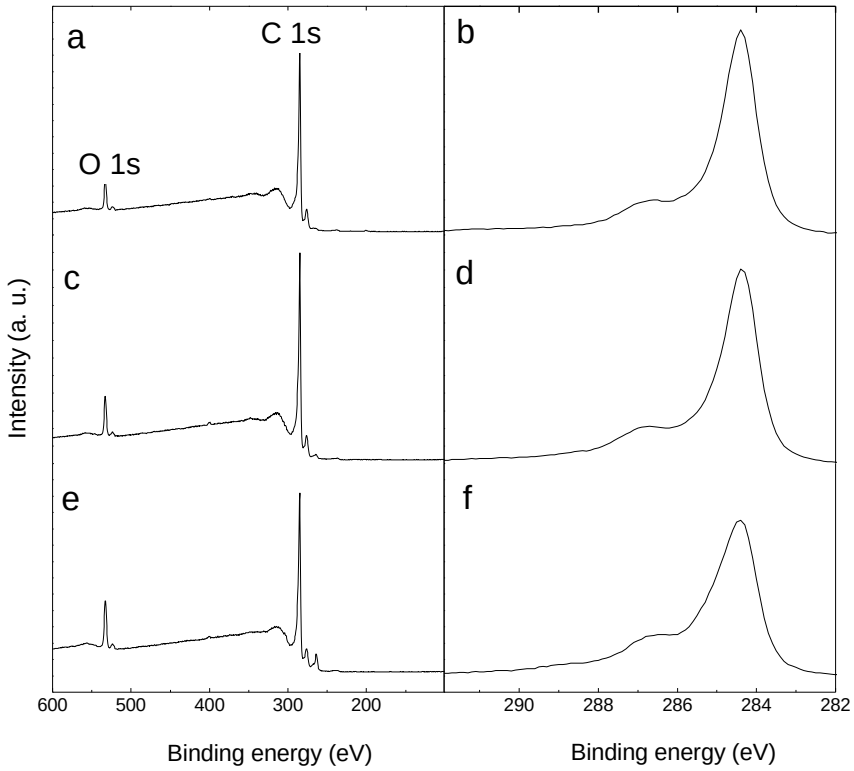

Figure 4. XPS survey spectra (a,c,e) and high resolution C 1s core level spectra (b,d,f) for graphene samples obtained by aqueous anodic exfoliation of graphite foil in 0.05 M NaCl (a,b), 0.1 M NaBr (c,d) and 0.1 M NaI (e,f).

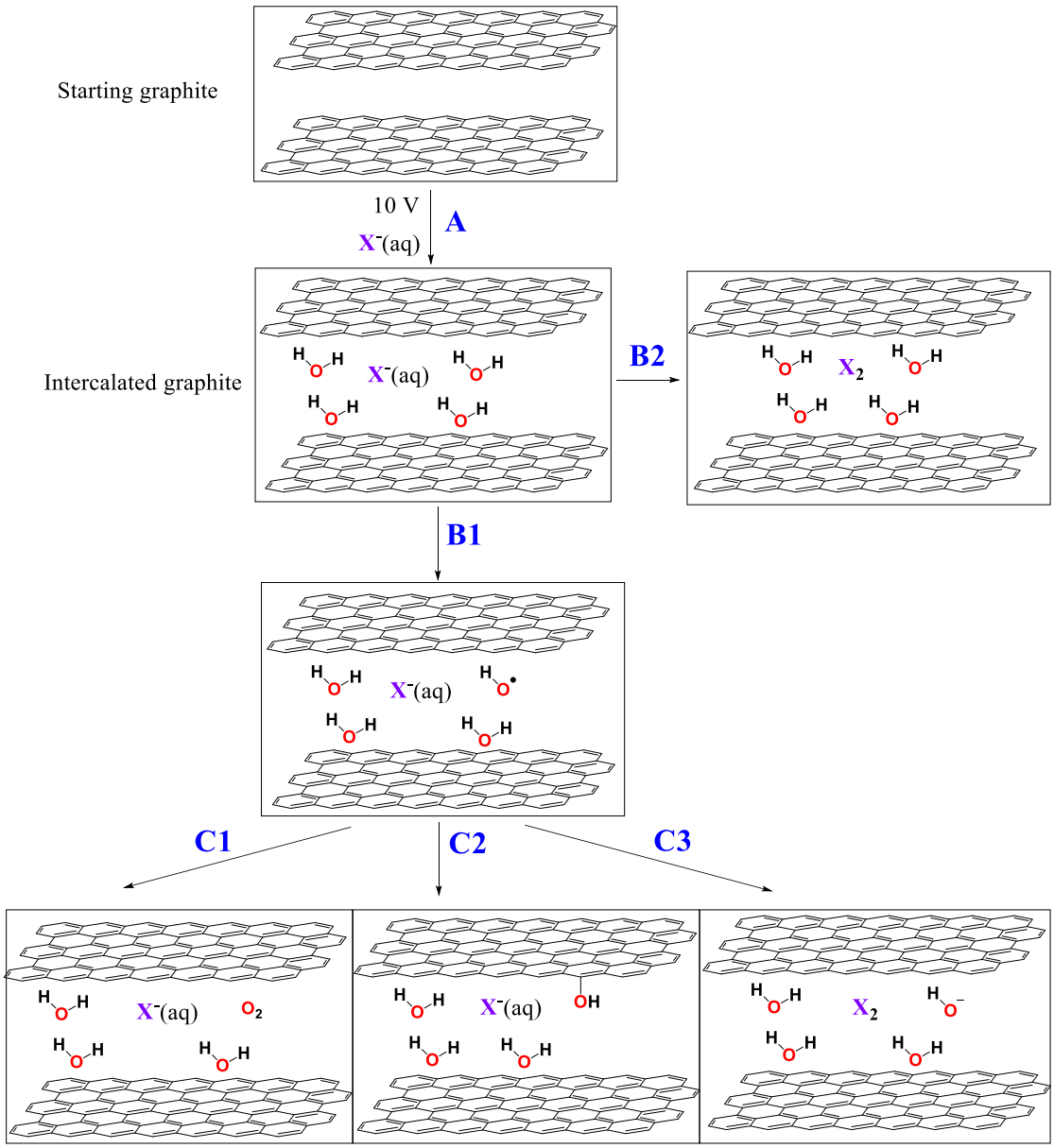

Figure 5. Schematic chart depicting the possible redox processes that take place when halide anions ($X^- \equiv Cl^-$, Br^- or I^-) are used as electrolyte in the aqueous anodic exfoliation of graphite. Step A: intercalation of hydrated halide [X^-(aq)] anions in the interlayer space of graphite. B1: anodic oxidation of intercalated water molecules to give ·OH radicals. B2: anodic oxidation of intercalated halide anions to give X_2 molecules. C1: further oxidation of ·OH radicals to give O_2 molecules. C2: attack of the graphitic lattice by ·OH radicals to give oxidized graphene materials. C3: neutralization of the highly reactive ·OH radicals by reaction with halide anions.

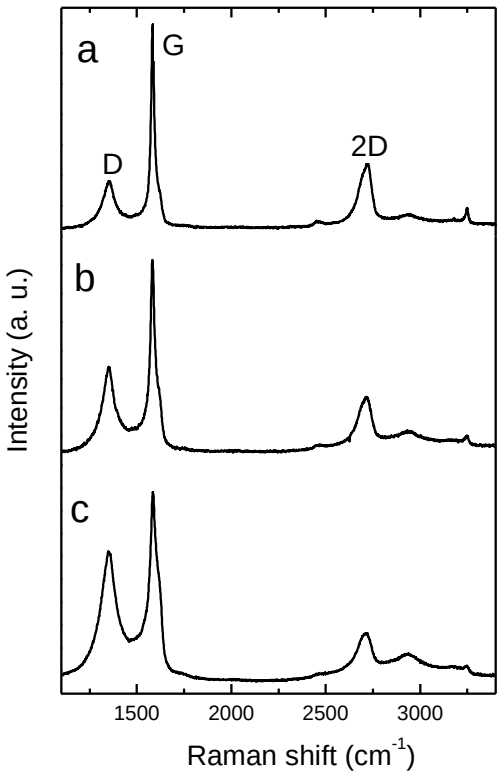

Figure 6. Raman spectra of graphene samples prepared by aqueous anodic exfoliation of graphite foil in 0.05 M NaCl (a), 0.1 M NaBr (b) and 0.1 M NaI (c).

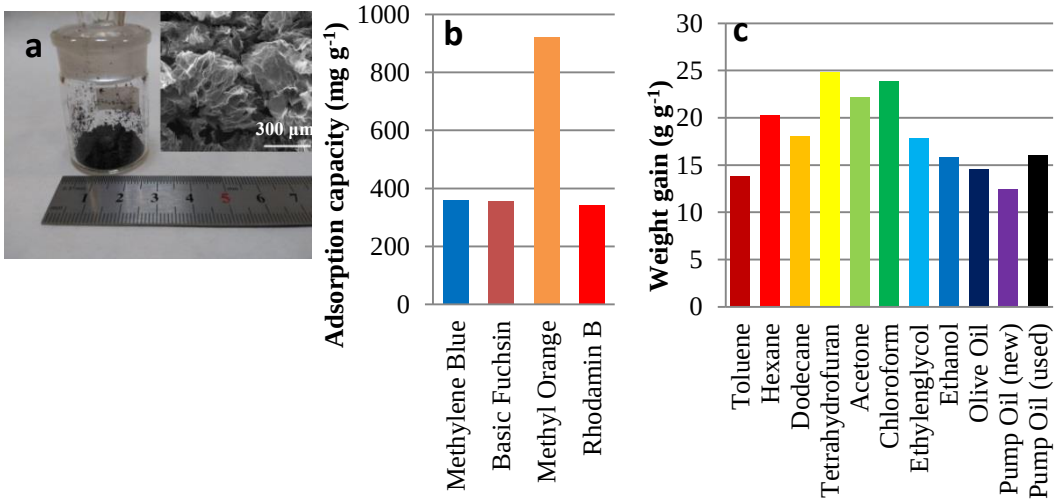

Figure 7. Digital photograph of as-prepared anodically exfoliated graphene using 0.1M NaI as electrolyte (a), SEM image of the same material (inset), adsorption capacities of this material for different dyes (b) and weight gains of the material for different solvents and oils (c).

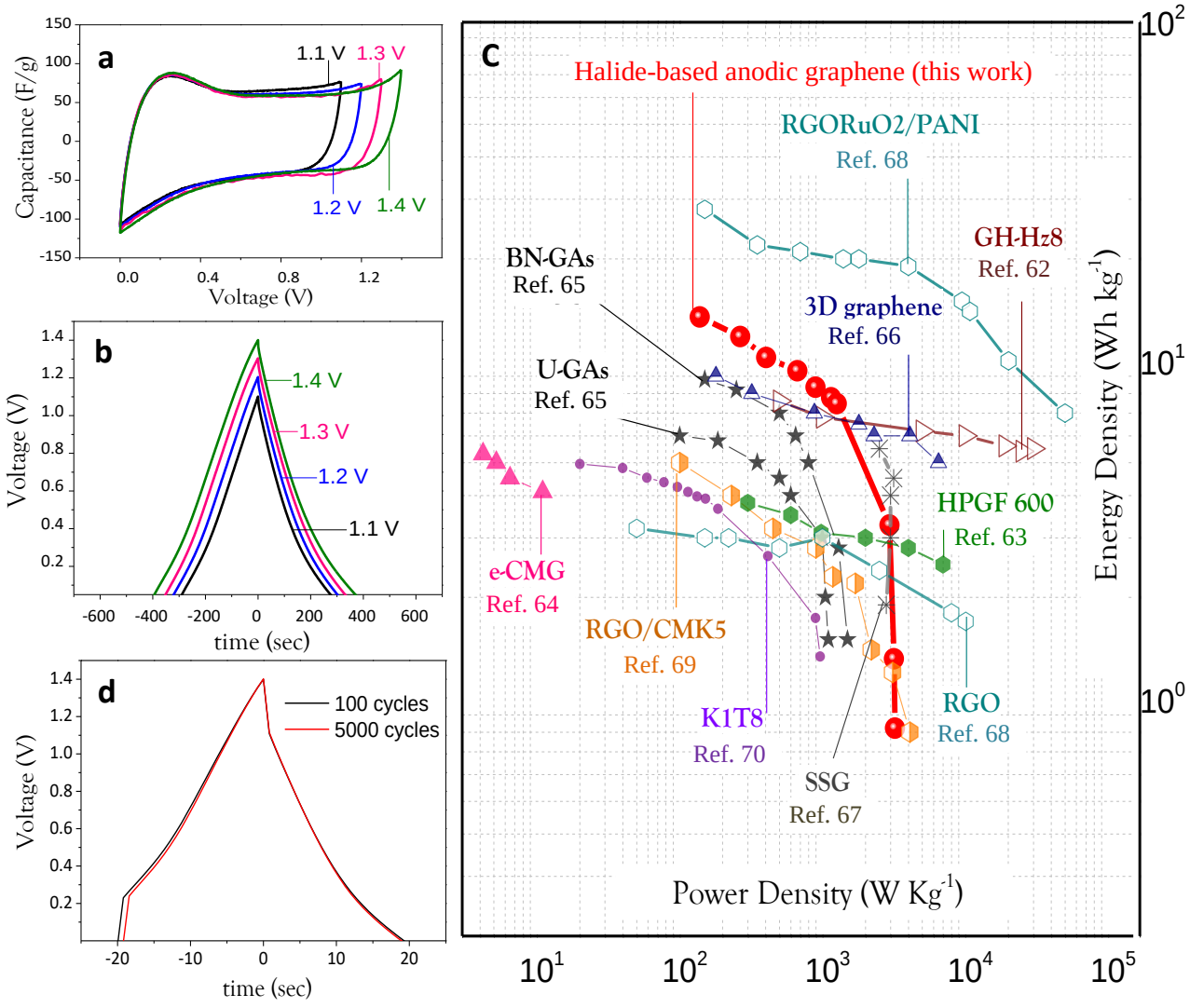

Figure 8. Supercapacitor performance tests for the halide-exfoliated graphite foil (0.1M NaI); a) cyclic voltammetry curves and b)galvanostatic charge-discharge profiles at different potential windows, c) Ragone plot for the exfoliated graphite and for some representative graphene-derived porous structures and d) cycling stability of the symmetric supercapacitor at 1 A/g over 2500 cycles.

Table of contents graphic

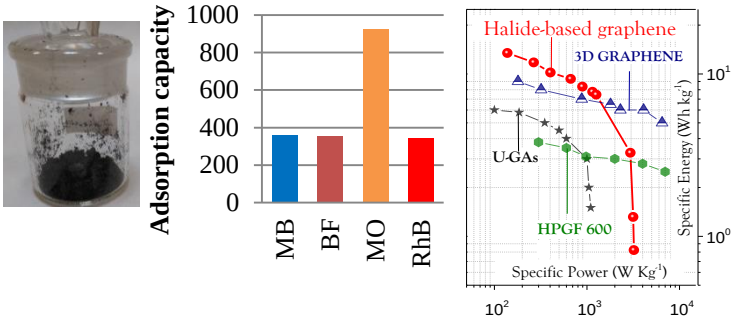

References

1 Ferrari, A. C.; Bonaccorso, F.; Fal'ko, V.; Novoselov, K. S.; Roche, S.; Boggild, P.; Borini, S.; Koppens, F. H. L.; Palermo, V.; Pugno, N.; Garrido, J. A.; Sordan, R.; Bianco, A.; Ballerini, L.; Prato, M.; Lidorikis, E.; Kivioja, J.; Marinelli, C.; Ryhanen, T.; Morpurgo, A.; Coleman, J. N.; Nicolosi, V.; Colombo, L.; Fert, A.; Garcia-Hernandez, M.; Bachtold, A.; Schneider, G. F.; Guinea, F.; Dekker, C.; Barbone, M.; Sun, Z.; Galiotis, C.; Grigorenko, A. N.; Konstantatos, G.; Kis, A.; Katsnelson, M.; Vandersypen, L.; Loiseau, A.; Morandi, V.; Neumaier, D.; Treossi, E.; Pellegrini, V.; Polini, M.; Tredicucci, A.; Williams, G. M.; Hee Hong, B.; Ahn, J.-H.; Min Kim, J.; Zirath, H.; van Wees, B. J.; van der Zant, H.; Occhipinti, L.; Di Matteo, A.; Kinloch, I. A.; Seyller, T.; Quesnel, E.; Feng, X.; Teo, K.; Rupesinghe, N.; Hakonen, P.; Neil, S. R. T.; Tannock, Q.; Lofwander, T.; Kinaret, J. Science and Technology Roadmap for Graphene, Related Two-Dimensional Crystals, and Hybrid Systems. *Nanoscale* **2015**, *7*, 4598-4810.

2 Zhang, Y.; Zhang, L.; Zhou, C. Review of Chemical Vapor Deposition of Graphene and Related Applications. *Acc. Chem. Res.* **2013**, *46*, 2329-2339.

3 Zhong, Y. L.; Tian, Z.; Simon, G. P.; Li, D. Scalable Production of Graphene Via Wet Chemistry: Progress and Challenges. *Mater. Today* **2015**, *18*, 73-78.

4 Du, W.; Jiang, X.; Zhu, L. From Graphite to Graphene: Direct Liquid-Phase Exfoliation of Graphite to Produce Single- and Few-Layered Pristine Graphene. *J. Mater. Chem. A* **2013**, *1*, 10592-10606.

5 Chen, L.; Xu, Z.; Li, j.; Li, Y.; Shan, M.; Wang, C.; Wang, Z.; Guo, Q.; Liu, L.; Chen, G.; Qian, X. A Facile Strategy to Prepare Functionalized Graphene Via Intercalation, Grafting and Self-Exfoliation of Graphite Oxide. *J. Mater. Chem.* **2012**, *22*, 13460-13463

6 Pei, S.; Cheng, H.-M. The Reduction of Graphene Oxide. *Carbon* **2012**, *50*, 3210-3228.

7 Niu, L.; Coleman, J. N.; Zhang, H.; Shin, H.; Chhowalla, M.; Zheng, Z. Production of Two-Dimensional Nanomaterials Via Liquid-Based Direct Exfoliation. *Small* **2016**, *12*, 272-293

8 Abdelkader, A. M.; Cooper, A. J.; Dryfe, R. A. W.; Kinloch, I. A. How to Get Between the Sheets: a Review of Recent Works on the Electrochemical Exfoliation of Graphene Materials from Bulk Graphite. *Nanoscale* **2015**, *7*, 6944-6956.

9 Yang, S.; Lohe, M. R.; Müllen, K.; Feng, X. New-Generation Graphene from Electrochemical Approaches: Production and Applications. *Adv. Mater.* **2016**, *28*, 6213-6221.

10 Abdelkader, A. M.; Kinloch, I. A.; Dryfe, R. A. W. Continuous Electrochemical Exfoliation of Micrometer-Sized Graphene Using Synergistic Ion Intercalations and Organic Solvents. *ACS Appl. Mater. Interfaces* **2014**, *6*, 1632-1639.

11 Cooper, A. J.; Wilson, N. R.; Kinloch, I. A.; Dryfe, R. A. W. Single Stage Electrochemical Exfoliation Method for the Production of Few-Layer Graphene Via Intercalation of Tetraalkylammonium Cations. *Carbon* **2014**, *66*, 340-350.

12 Ali Reza Kamali, A. R., Fraya, D. J. Large-Scale Preparation of Graphene by High Temperature Insertion of Hydrogen into Graphite. *Nanoscale*, **2015**, ***7***, 11310-11320

13 Kim, H. K.; Kamali, A. R.; Roh, K. C.; Kim, K. B.; Fray, D. J. Dual Coexisting Interconnected Graphene Nanostructures for High Performance Supercapacitor Applications. *Energy Environ. Sci*. **2016**, *9*, 2249-2256

14 Abdelkader, A. M.; Patten, H. V.; Li, Z.; Chen, Y.; Kinloch, I. A. Electrochemical Exfoliation of Graphite in Quaternary Ammonium-Based Deep Eutectic Solvents: a Route for the Mass Production of Graphane. *Nanoscale*, **2015**, *7*, 11386-11392

15 Lu, J.; Yang, J.-x.; Wang, J.; Lim, A.; Wang, S.; Loh, K. P. One-Pot Synthesis of Fluorescent Carbon Nanoribbons, Nanoparticles, and Graphene by the Exfoliation of Graphite in Ionic Liquids. *ACS Nano* **2009**, *3*, 2367-2375.

16 Su, C.-Y.; Lu, A.-Y.; Xu, Y.; Chen, F.-R.; Khlobystov, A. N.; Li, L.-J. High-Quality Thin Graphene Films from Fast Electrochemical Exfoliation. *ACS Nano* **2011**, *5*, 2332-2339.

17 Parvez, K.; Wu, Z.-S.; Li, R.; Liu, X.; Graf, R.; Feng, X.; Müllen, K. Exfoliation of Graphite into Graphene in Aqueous Solutions of Inorganic Salts. *J. Am. Chem. Soc.* **2014**, *136*, 6083-6091.

18 Munuera, J. M.; Paredes, J. I.; Villar-Rodil, S.; Ayán-Varela, M.; Pagán, A.; Aznar-Cervantes, S. D.; Cenis, J. L.; Martínez-Alonso, A.; Tascón, J. M. D. High Quality, Low Oxygen Content and Biocompatible Graphene Nanosheets Obtained by Anodic Exfoliation of Different Graphite Types. *Carbon* **2015**, *94*, 729-739.

19 Najafabadi, A. T.; Gyenge, E. Synergistic Production of Graphene Microsheets by Simultaneous Anodic and Cathodic Electro-Exfoliation of Graphitic Electrodes in Aprotic Ionic Liquids. *Carbon*, **2015**, *84*, 449-459

20 Najafabadi, A. T.; Ng, N.; Gyenge, E. High-Yield Graphene Production by Electrochemical Exfoliation of Graphite: Novel Ionic liquid (IL)–Acetonitrile Electrolyte With Low IL Content. *Carbon*, **2014**, *71*, 58-69

21 Najafabadi, A. T.; Gyenge, E. Electrochemically Exfoliated Graphene Anodes with Enhanced Biocurrent Production in Single-Chamber Air-Breathing Microbial Fuel Cells. *Biosens. Bioelectron.* **2016**, *81*, 103-110

22 Ambrosi, A.; Pumera, M. Electrochemically Exfoliated Graphene and Graphene Oxide for Energy Storage and Electrochemistry Applications. *Chem. - Eur. J.* **2016**, *22*, 153-159.

23 Liu, J.; Poh, C. K.; Zhan, D.; Lai, L.; Lim, S. H.; Wang, L.; Liu, X.; Gopal Sahoo, N.; Li, C.; Shen, Z.; Lin, J. Improved Synthesis of Graphene Flakes From the Multiple Electrochemical Exfoliation of Graphite Rod. *Nano Energy* **2013**, *2*, 377-386.

24 Wu, L.; Li, W.; Li, P.; Liao, S.; Qiu, S.; Chen, M.; Guo, Y.; Li, Q.; Zhu, C.; Liu, L. Powder, Paper and Foam of Few-Layer Graphene Prepared in High Yield by Electrochemical Intercalation Exfoliation of Expanded Graphite. *Small* **2014**, *10*, 1421-1429.

25 Abdelkader, A. M.; Kinloch, I. A.; Dryfe, R. A. W. High-Yield Electro-Oxidative Preparation of Graphene Oxide. *Chem. Commun.* **2014**, *50*, 8402-8404.

26 Chuang, C.-H.; Su, C.-Y.; Hsu, K.-T.; Chen, C.-H.; Huang, C.-H.; Chu, C.-W.; Liu, W.-R. A Green, Simple and Cost-Effective Approach to Synthesize High Quality Graphene by Electrochemical Exfoliation Via Process Optimization. *RSC Adv.* **2015**, *5*, 54762-54768.

27 Paredes, J. I.; Munuera, J. M. Recent Advances and Energy-Related Applications of High Quality/Chemically Doped Graphenes Obtained by Electrochemical Exfoliation Methods. *J. Mater. Chem. A* **2017**, *5*, 7228-7242.

28 Chen, C.-H.; Yang, S.-W.; Chuang, M.-C.; Woon, W.-Y.; Su, C.-Y. Towards the Continuous Production of High Crystallinity Graphene Via Electrochemical Exfoliation with Molecular In Situ Encapsulation. *Nanoscale* **2015**, *7*, 15362-15373.

29 Yang, S.; Brüller, S.; Wu, Z.-S.; Liu, Z.; Parvez, K.; Dong, R.; Richard, F.; Samorì, P.; Feng, X.; Müllen, K. Organic Radical-Assisted Electrochemical Exfoliation for the

Scalable Production of High-Quality Graphene. *J. Am. Chem. Soc.* **2015**, *137*, 13927-13932.

30 Munuera, J. M.; Paredes, J. I.; Villar-Rodil, S.; Ayán-Varela, M.; Martínez-Alonso, A.; Tascón, J. M. D. Electrolytic Exfoliation of Graphite in Water with Multifunctional Electrolytes: En Route Towards High Quality, Oxide-Free Graphene Flakes. *Nanoscale* **2016**, *8*, 2982-2998.

31 Gaier, J. R.; Ditmars, N. F.; Dillon, A. R. Aqueous Electrochemical Intercalation of Bromine into Graphite Fibers. *Carbon* **2005**, *43*, 189-193.

32 Niu, L.; Li, M.; Tao, X.; Xie, Z.; Zhou, X.; Raju, A. P. A.; Young, R. J.; Zheng, Z. Salt-Assisted Direct Exfoliation of Graphite Into High-Quality, Large-Size, Few-Layer Graphene Sheets. *Nanoscale* **2013**, *5*, 7202-7208.

33 Munaiah, Y.; Ragupathy, P.; Pillai, V. K. Single-Step Synthesis of Halogenated Graphene through Electrochemical Exfoliation and Its Utilization as Electrodes for Zinc Bromine Redox Flow Battery. *J. Electrochem. Soc.* **2016**, *163*, A2899-A2910.

34 Ayán-Varela, M.; Paredes, J. I.; Guardia, L.; Villar-Rodil, S.; Munuera, J. M.; Díaz-González, M.; Fernández-Sánchez, C.; Martínez-Alonso, A.; Tascón, J. M. D. Achieving Extremely Concentrated Aqueous Dispersions of Graphene Flakes and Catalytically Efficient Graphene-Metal Nanoparticle Hybrids with Flavin Mononucleotide as a High-Performance Stabilizer. *ACS Appl. Mater. Interfaces* **2015**, *7*, 10293-10307.

35 Guardia, L.; Fernández-Merino, M. J.; Paredes, J. I.; Solís-Fernández, P.; Villar-Rodil, S.; Martínez-Alonso, A.; Tascón, J. M. D. High-Throughput Production of Pristine Graphene in an Aqueous Dispersion Assisted by Non-Ionic Surfactants. *Carbon* **2011**, *49*, 1653-1662.

36 Nemes-Incze, P.; Osváth, Z.; Kamarás, K.; Biró, L. P. Anomalies in Thickness Measurements of Graphene and Few Layer Graphite Crystals by Tapping Mode Atomic Force Microscopy. *Carbon* **2008**, *46*, 1435-1442.

37 Xuhua, H.; Senlin, L.; Zhiqiang, Q.; Wei, Z.; Wei, Y.; Yanyan, F. Low Defect Concentration Few-Layer Graphene Using a Two-Step Electrochemical Exfoliation. *Nanotechnology* **2015**, *26*, 105602-105608

38 Lou, F.; Buan, M. E. M.; Muthuswamy, N.; Walmsley, J. C.; Ronning, M.; Chen, D. One-Step Electrochemical Synthesis of Tunable Nitrogen-Doped Graphene. *J. Mater. Chem. A* **2016**, *4*, 1233-1243.

39 Wei, W.; Wang, G.; Yang, S.; Feng, X.; Müllen, K. Efficient Coupling of Nanoparticles to Electrochemically Exfoliated Graphene. *J. Am. Chem. Soc.* **2015**, *137*, 5576-5581.

40 Mancinelli, R.; Botti, A.; Bruni, F.; Ricci, M. A.; Soper, A. K. Hydration of Sodium, Potassium, and Chloride Ions in Solution and the Concept of Structure Maker/Breaker. *J. Phys. Chem. B* **2007**, *111*, 13570-13577.

41 D'Angelo, P.; Migliorati, V.; Guidoni, L. Hydration Properties of the Bromide Aqua Ion: the Interplay of First Principle and Classical Molecular Dynamics, and X-ray Absorption Spectroscopy. *Inorg. Chem.* **2010**, *49*, 4224-4231.

42 Fulton, J. L.; Schenter, G. K.; Baer, M. D.; Mundy, C. J.; Dang, L. X.; Balasubramanian, M. Probing the Hydration Structure of Polarizable Halides: A Multiedge XAFS and Molecular Dynamics Study of the Iodide Anion. *J. Phys. Chem. B* **2010**, *114*, 12926-12937.

43 Foote, S. C.; Valentine, J. S.; Greenberg, A.; Liebman, J. F. Active Oxygen in Chemistry, 1st ed.; Chapman & Hall: Glasgow, 1995.

44 Vanýsek, P., CRC Handbook of Chemistry and Physics, 93rd ed.; CRC Press: Boca Raton, 2012.

45 Jayson, G. G.; Parsons, B. J.; Swallow, A. J. Some Simple, Highly Reactive, Inorganic Chlorine Derivatives in Aqueous Solution. Their Formation Using Pulses of Radiation and Their Role in the Mechanism of the Fricke Dosimeter. *J. Chem. Soc., Faraday Trans.1* **1973**, *69*, 1597-1607.

46 Zehavi, D.; Rabani, J. Oxidation of Aqueous Bromide Ions by Hydroxyl Radicals. Pulse Radiolytic Investigation. *J. Phys. Chem.* **1972**, *76*, 312-319.

47 Thomas, J. K. Rates of Reaction of the Hydroxyl Radical. *Trans. Faraday Soc*. **1965**, *61*, 702-707.

48 Ferrari, A. C.; Basko, D. M. Raman Spectroscopy as a Versatile Tool for Studying the Properties of Graphene. *Nat. Nanotechnol*. **2013**, *8*, 235-246.

49 Lotya, M.; Hernandez, Y.; King, P. J.; Smith, R. J.; Nicolosi, V.; Karlsson, L. S.; Blighe, F. M.; De, S.; Wang, Z.; McGovern, I. T.; Duesberg, G. S.; Coleman, J. N. Liquid Phase Production of Graphene by Exfoliation of Graphite in Surfactant/Water Solutions. *J. Am. Chem. Soc.* **2009**, *131*, 3611-3620.

50 De, S.; King, P. J.; Lotya, M.; O'Neill, A.; Doherty, E. M.; Hernandez, Y.; Duesberg, G. S.; Coleman, J. N. Flexible, Transparent, Conducting Films of Randomly Stacked Graphene from Surfactant-Stabilized, Oxide-Free Graphene Dispersions. *Small* **2010**, *6*, 458-464.

51 Sun, Z.; Masa, J.; Liu, Z.; Schuhmann, W.; Muhler, M. Highly Concentrated Aqueous Dispersions of Graphene Exfoliated by Sodium Taurodeoxycholate: Dispersion Behavior

and Potential Application as a Catalyst Support for the Oxygen-Reduction Reaction. *Chem. - Eur. J.* **2012**, *18*, 6972-6978.

52 Chabot, V.; Kim, B.; Sloper, B.; Tzoganakis, C.; Yu, A. High Yield Production and Purification of Few Layer Graphene by Gum Arabic Assisted Physical Sonication. *Sci. Rep.* **2013**, *3*, 1378-1385

53 Perreault, F.; Fonseca de Faria, A.; Elimelech, M. Environmental Applications of Graphene-Based Nanomaterials. *Chem. Soc. Rev.* **2015**, *44*, 5861-5896.

54 Raccichini, R.; Varzi, A.; Passerini, S.; Scrosati, B. The Role of Graphene for Electrochemical Energy Storage. *Nat. Mater.* **2015**, *14*, 271-279.

55 Sherrell, P. C.; Mattevi, C. Mesoscale Design of Multifunctional 3D Graphene Networks. *Mater. Today* **2016**, *19*, 428-436.

56 Chen, B.; Ma, Q.; Tan, C.; Lim, T.-T.; Huang, L.; Zhang, H. Carbon-Based Sorbents with Three-Dimensional Architectures for Water Remediation. *Small* **2015**, *11*, 3319-3336.

57 Li, F.; Jiang, X.; Zhao, J.; Zhang, S. Graphene Oxide: A Promising Nanomaterial for Energy and Environmental Applications. *Nano Energy* **2015**, *16*, 488-515.

58 Wang, H.; Yuan, X.; Zeng, G.; Wu, Y.; Liu, Y.; Jiang, Q.; Gu, S. Three Dimensional Graphene Based Materials: Synthesis and Applications from Energy Storage and Conversion to Electrochemical Sensor and Environmental Remediation. *Adv. Colloid Interface Sci.* **2015**, *221*, 41-59.

59 Munuera, J. M.; Paredes, J. I.; Villar-Rodil, S.; Martínez-Alonso, A.; Tascón, J. M. D. A Simple Strategy to Improve the Yield of Graphene Nanosheets in the Anodic Exfoliation of Graphite Foil. *Carbon* **2017**, *115*, 625-628.

60 Wan, W.; Lin, Y.; Prakash, A.; Zhou, Y. Three-Dimensional Carbon-Based Architectures for Oil Remediation: From Synthesis and Modification to Functionalization. *J. Mater. Chem. A* **2016**, *4*, 18687-18705.

61 Dai, Z.; Peng, C.; Chae, J. H.; Ng, K. C.; Chen, G. Z. Cell Voltage Versus Electrode Potential Range in Aqueous Supercapacitors. *Sci. Rep.* **2015**, *5*, 9854-9862.

62 Zhang, L.; Shi, G. Preparation of Highly Conductive Graphene Hydrogels for Fabricating Supercapacitors with High Rate Capability. *J. Phys. Chem. C* **2011**, *115*, 17206-17212.

63 Zuo, Z.; Kim, T. Y.; Kholmanov, I.; Li, H.; Chou, H.; Li, Y. Ultra-light Hierarchical Graphene Electrode for Binder-Free Supercapacitors and Lithium-Ion Battery Anodes. *Small* **2015**, *11*, 4922-4930.

64 Choi, B. G.; Yang, M.; Hong, W. H.; Choi, J. W.; Huh, Y. S. 3D Macroporous Graphene Frameworks for Supercapacitors with High Energy and Power Densities. *ACS Nano* **2012**, *6*, 4020-4028.

65 Wu, Z.-S.; Winter, A.; Chen, L.; Sun, Y.; Turchanin, A.; Feng, X.; Müllen, K. Three-Dimensional Nitrogen and Boron Co-doped Graphene for High-Performance All-Solid-State Supercapacitors. *Adv. Mater*. **2012**, *24*, 5130-5135.

66 Ramadoss, A.; Yoon, K.-Y.; Kwak, M.-J.; Kim, S.-I.; Ryu, S.-T.; Jang, J.-H. Fully Flexible, Lightweight, High Performance All-Solid-State Supercapacitor Based on 3-Dimensional-Graphene/Graphite-Paper. *J. Power Sources* **2017**, *337*, 159-165.

67 Yang, X.; Zhu, J.; Qiu, L.; Li, D. Bioinspired Effective Prevention of Restacking in Multilayered Graphene Films: Towards the Next Generation of High-Performance Supercapacitors. *Adv. Mater.* **2011**, *23*, 2833-2838.

68 Zhang, J.; Jiang, J.; Li, H.; Zhao, X. S. A High-Performance Asymmetric Supercapacitor Fabricated with Graphene-Based Electrodes. *Energy Environ. Sci.* **2011**, *4*, 4009-4015.

69 Lei, Z.; Liu, Z.; Wang, H.; Sun, X.; Lu, L.; Zhao, X. S. A High-Energy-Density Supercapacitor with Graphene-CMK-5 as the Electrode and Ionic Liquid as the Electrolyte. *J. Mater. Chem. A* **2013**, *1*, 2313-2321.

70 Enterría, M.; Martín-Jimeno, F. J.; Suárez-García, F.; Paredes, J. I.; Pereira, M. F. R.; Martins, J. I.; Martínez-Alonso, A.; Tascón, J. M. D.; Figueiredo, J. L. Effect of Nanostructure on the Supercapacitor Performance of Activated Carbon Xerogels Obtained from Hydrothermally Carbonized Glucose-Graphene Oxide Hybrids. *Carbon* **2016**, *105*, 474-483.